

## A general framework for evaluating nonlinearity, noise and dynamic range in continuous-time OTA-C filters for computer-aided design and optimization

S. Koziel<sup>1,\*</sup>,<sup>†</sup>, A. Ramachandran<sup>2</sup>, S. Szczepanski<sup>3</sup> and E. Sánchez-Sinencio<sup>2</sup>

<sup>1</sup>*Simulation Optimization Systems Research Laboratory, Department of Electrical and Computer Engineering, McMaster University, Hamilton, Ont., Canada L8S 4K1*

<sup>2</sup>*Department of Electrical Engineering Texas A&M University, College Station, TX 77843, U.S.A.*

<sup>3</sup>*Faculty of Electronics, Telecommunications and Informatics, Gdansk University of Technology, Gdansk 80-952, Poland*

### SUMMARY

Efficient procedures for evaluating nonlinear distortion and noise valid for any OTA-C filter of arbitrary order are developed based on matrix description of a general OTA-C filter model. Since those procedures use OTA macromodels, they allow us to obtain the results significantly faster than transistor-level simulation. On the other hand, the general OTA-C filter model allows us to apply matrix transforms that manipulate (rescale) filter element values and/or change topology without changing its transfer function. Due to this, the proposed procedures can be used in direct optimization of OTA-C filters with respect to important characteristics such as noise performance, THD, IM3, DR or SNR. As an example, a simple optimization procedure using equivalence transformations is discussed. An application example of the proposed approach to optimal block sequencing and gain distribution of 8th order cascade Butterworth filter is given. Accuracy of the theoretical tools has been verified by comparing to transistor-level simulation results and to experimental results. Copyright © 2006 John Wiley & Sons, Ltd.

Received 11 October 2005; Revised 22 August 2006

KEY WORDS: OTA-C filters; nonlinear distortion analysis; noise analysis; CAD; performance optimization

### 1. INTRODUCTION

Continuous-time analog filters and equalizers based on transconductance amplifiers and capacitors (OTA-C filters) are suitable solutions for various voltage-mode and current-mode signal-processing tasks over wide frequency ranges. In recent years, continuous-time OTA-C filters, often realized

\*Correspondence to: S. Koziel, Simulation Optimization Systems Research Laboratory, Department of Electrical and Computer Engineering, McMaster University, Hamilton, Ont., Canada L8S 4K1.

<sup>†</sup>E-mail: koziels@mcmaster.ca

as integrated circuits (ICs), have received considerable attention in various applications, such as hard-disc drives, video filters, wireless communications, computer systems, biomedical circuits, and control and instrumentation systems [1–12].

The literature has a rich collection of various synthesis and design methods for different types and architectures of the continuous time OTA-C filters [1, 2, 13–21]. Sun *et al.* [20] have introduced the synthesis and performance analysis of canonical integrator based inverse feedback (IFLF) filters. The authors have addressed a particular class of OTA-C structures and have discussed the design issues related to it. In [1, 21], a new universal method of synthesis and analysis of any filter of arbitrary order have been developed based on the matrix description of a general OTA-C filter model. The advantages of this approach and the utility value are further mentioned and utilized in Section 2.

The main attractions of OTA-C filters is their excellent high-frequency performance, but many of their other properties still need improving, among them are operation at reduced supply voltages and power consumption, less dependence on parasitic effects, lower noise level, better linearity and wider dynamic range. A large number of research papers have been published which deal with improving performance of the OTA-C filters focusing on the dynamic range, THD, and noise [8–12, 22–30]. Some of the papers include estimation of dynamic range [4, 31], nonlinear distortion using Volterra series approach [32–34] and harmonic injection method [35], as well as noise [36–39]. In this paper, based on the matrix description of the general OTA-C filter class [1], the estimation of nonlinear distortion, noise, and dynamic range has been proposed.

The most challenging task for the analog design engineers is to have efficient tools for nonlinear distortion and noise analysis, in particular, tools that can be embedded into computer-aided filter-design systems. This would help the designer to improve and optimize the performance parameters of the filters and also explore innovative designs. The literature has a wide range of computer-aided tools to assist the design of digital circuits. However, the resources for analog design is limited. A survey indicates research material [5–7] which presents some of the computer aided design (CAD) tools for analog circuits. In [5], the synthesis and analysis of analog circuits are based on determinant decision diagrams. In [6] the authors proposed a computer-aided circuit analysis tool for radio frequency-integrated circuits. A CAD tool for the synthesis of linear analog functions with a network of OTAs has been proposed in [7]. The approach is however more focused on the design or the synthesis of the analog filters and not dealing with the performance parameters and their optimization.

The need of the hour is a CAD tool, which can take into consideration various alternative structures of any arbitrary order OTA-C filter, optimized for various performance parameters like the total harmonic distortion, output noise, dynamic range and sensitivity. The main requirements for such tools are that they have to be general (so that the same evaluation formulas and software packages can be used to handle all possible filter topologies) and fast enough to be integrated with numerical optimization algorithms. This is the basic motivation for the research mentioned in this paper.

In this work, the above-mentioned requirements are satisfied by deriving our analysis tools and evaluation formulas from the general OTA-C filter model [1] that uses nonlinear OTA macromodels. As we show in the subsequent sections, they allow us to obtain the results significantly faster than transistor-level simulation. In case of transient analysis, the speed-up may be as much as three orders of magnitude with almost no loss of accuracy. This makes it possible to carry out direct numerical optimization of OTA-C filters with respect to important characteristics including noise performance, nonlinear distortion and dynamic range. On the other hand, the general OTA-C

filter model allows us to apply matrix transforms that manipulate (rescale) filter element values and/or change topology without changing its transfer function. The above features can be a basis to build automated optimization procedures for OTA-C filters. In particular, we discuss a simple optimization procedure using equivalence transformations. Suitable software package is also implemented.

The paper is organized as follows. In Section 2 a general structure of OTA-C filter with nonlinear transconductors is introduced. A nonlinear ordinary differential system that describes the time evolution of the voltage signals at the intrinsic nodes of the filter as well as the output signal of the filter is derived. This system can be integrated numerically provided that the macromodel of transconductor in the form of analytical description of its transfer function is given. In Section 3, the noise analysis of the general OTA-C filter model is performed, which leads to explicit and compact expressions for the output and input-referred noise spectra of any OTA-C filter. Verification of the proposed approach is given in Section 4 by comparing the model results of Sections 2 and 3 to SPICE simulations as well as to experimental results (using a 5th order Bessel filter that was fabricated in 0.5  $\mu\text{m}$  CMOS process). Section 5 describes a simple optimization procedure based on matrix transformations of the general filter model. An application example of the proposed approach to performance optimization of an 8th order cascade Butterworth filter is discussed. Remarks and conclusions are contained in Section 6.

## 2. DYNAMICS OF NONLINEAR OTA-C FILTERS

Consider a general structure of a voltage-mode OTA-C filter shown in Figure 1. The current-mode counterpart can be obtained by inverting all transconductors and interchanging input and output of the filter [30, 31]. The structure in Figure 1 contains  $n$  internal nodes denoted as  $x_i$ ,  $i = 1, \dots, n$ ,  $n$  input transconductors  $G_{bi}$ , an output summer consisting of summing transconductors  $G_{ci}$  feedback transconductor  $G_o$ , and a feedforward transconductor  $G_d$ , as well as a set of feedback and feedforward transconductors  $G_{ij}$ . We assume that in general transconductors are not linear. All transconductors form *active network*, while input capacitors  $C_{bi}$ ,  $i = 1, \dots, n$  and capacitors  $C_{ij}$ ,  $1 \leq i < j \leq n$  form *passive network*. We assume capacitors to be linear, since in most practical filters inherent nonlinearities of capacitors can be neglected in comparison to those of active elements. It is easily seen that any OTA-C filter is a particular case of the general structure in Figure 1. Note also that  $n$  is not necessarily equal to the order of the filter transfer function [1].

Now we would like to derive an analytical description of the considered structure in the time domain. In the following considerations we will denote the voltage at the  $i$ th node  $x_i$  also by  $x_i$ , which will not lead to confusion. Symbols  $u_i$ ,  $u_o$  will denote the input and output voltages, respectively. The rest of the necessary notation is introduced in Figure 2.

According to the notation in Figure 2, the general structure of OTA-C filter in Figure 1 can be described by the following system of differential equations:

$$i_k(t) = C_{kk} \frac{dx_k(t)}{dt}, \quad k = 1, 2, \dots, n \quad (1)$$

$$i_{kl}(t) = C_{kl} \left( \frac{dx_k(t)}{dt} - \frac{dx_l(t)}{dt} \right), \quad k, l = 1, 2, \dots, n, \quad k < l \quad (2)$$

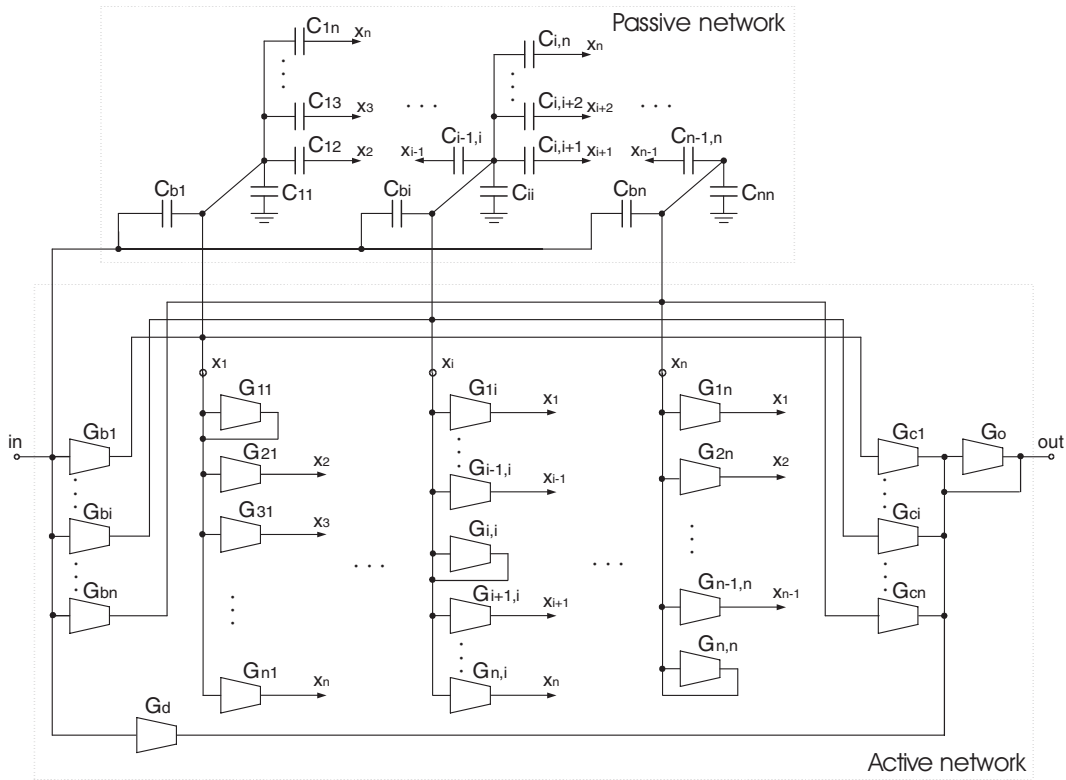


Figure 1. General structure of voltage-mode OTA-C filter with nonlinear transconductors.

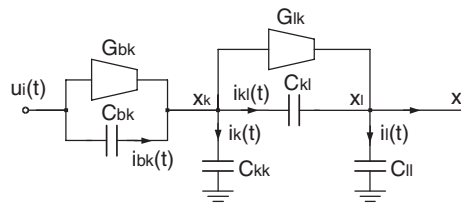


Figure 2. Part of the circuit in Figure 1 with the notation used to its analytical description.

$$i_{bk}(t) = C_{bk} \left( \frac{du_i(t)}{dt} - \frac{dx_k(t)}{dt} \right), \quad k = 1, 2, \dots, n \quad (3)$$

$$- \sum_{l=1, l \neq k}^n i_{lk}(t) + i_k(t) - i_{bk}(t) = \sum_{l=1}^n G_{kl}(x_l(t)) + G_{bk}(u_i(t)), \quad k = 1, 2, \dots, n \quad (4)$$

$$u_o(t) = -G_o^{-1} \left( \sum_{l=1}^n G_{cl}(x_l(t)) + G_d(u_i(t)) \right) \quad (5)$$

We assume the following initial conditions:

$$x_k(0) = x_{0k}, \quad k = 1, 2, \dots, n, \quad u_i(0) = u_{i0} \tag{6}$$

Note that  $G_{kl}, G_{bk}, G_{cl}, G_d$  and  $G_o, k, l = 1, 2, \dots, n$  are in general nonlinear functions of their input variables. Inserting (1)–(3) into (4) and denoting  $dx_k(t)/dt$  by  $x'_k(t)$  we obtain

$$\left( C_{bk} + \sum_{l=1}^n C_{lk} \right) x'_k(t) - \sum_{l=1, l \neq k}^n C_{lk} x'_l(t) = \sum_{l=1}^n G_{kl}(x_l(t)) + G_{bk}(u_i(t)) + C_{bk} u'_i(t) \tag{7}$$

for  $k = 1, 2, \dots, n$ . To simplify the notation, in Equation (7) we used symbols  $C_{kl}$  ( $k > l$ ) that denote the same elements as  $C_{lk}$ . Define vectors  $\mathbf{x}(t)$  and  $\mathbf{x}'(t)$  as

$$\mathbf{x}(t) = [x_1(t) \ \dots \ x_n(t)]^T, \quad \mathbf{x}'(t) = [x'_1(t) \ \dots \ x'_n(t)]^T, \quad \mathbf{x}_0 = [x_{01} \ \dots \ x_{0n}]^T \tag{8}$$

and (the indefinite admittance matrix) matrix  $\mathbf{T}_C$  as

$$\mathbf{T}_C = \begin{bmatrix} C_{b1} + \sum_{j=1}^n C_{1j} & -C_{12} & \dots & -C_{1n} \\ -C_{12} & C_{b2} + \sum_{j=1}^n C_{2j} & \dots & -C_{2n} \\ \vdots & \vdots & \ddots & \vdots \\ -C_{1n} & -C_{2n} & \dots & C_{bn} + \sum_{j=1}^n C_{nj} \end{bmatrix} \tag{9}$$

Then, system (5)–(7) can be written as below

$$\mathbf{T}_C \mathbf{x}'(t) = \mathbf{T}_C \begin{pmatrix} x'_1(t) \\ x'_2(t) \\ \vdots \\ x'_n(t) \end{pmatrix} = \begin{bmatrix} \sum_{l=1}^n G_{1l}(x_l(t)) \\ \sum_{l=1}^n G_{2l}(x_l(t)) \\ \vdots \\ \sum_{l=1}^n G_{nl}(x_l(t)) \end{bmatrix} + \begin{bmatrix} G_{b1}(u_i(t)) + C_{b1} u'_i(t) \\ G_{b2}(u_i(t)) + C_{b2} u'_i(t) \\ \vdots \\ G_{bn}(u_i(t)) + C_{bn} u'_i(t) \end{bmatrix} \tag{10}$$

$$u_o(t) = -G_o^{-1} \left( \sum_{l=1}^n G_{cl}(x_l(t)) + G_d(u_i(t)) \right), \quad \mathbf{x}(0) = \mathbf{x}_0, \quad u_i(0) = u_{i0} \tag{11}$$

Let us now consider a special case, where all transconductors are linear, i.e. we have  $G_{kl}(y) = G_{m.kly}, G_{bk}(y) = G_{m.bky}, G_{cl}(y) = G_{m.cly}, G_d(y) = G_{m.dy}$  and  $G_o(y) = G_{m.oy}, k, l = 1, 2, \dots, n$ .

Define the following matrices:

$$\mathbf{G} = \begin{bmatrix} G_{m.11} & \cdots & G_{m.1n} \\ \vdots & \ddots & \vdots \\ G_{m.n1} & \cdots & G_{m.nn} \end{bmatrix}, \quad \mathbf{C} = [c_1 \ \dots \ c_n] \quad (12)$$

$$\mathbf{B} = \left[ G_{m.b1} + C_{b1} \frac{d}{dt} \ \dots \ G_{m.bn} + C_{bn} \frac{d}{dt} \right]^T, \quad \mathbf{D} = d \quad (13)$$

with  $c_i = -G_{m.ci}/G_{mo}$ ,  $i = 1, 2, \dots, n$  and  $d = -G_{md}/G_{mo}$ . Using this notation we can rewrite Equations (10), (11) in the following way:

$$\begin{aligned} \mathbf{T}_C \mathbf{x}'(t) &= \mathbf{G}\mathbf{x}(t) + \mathbf{B}u_i(t), & \mathbf{x}(0) &= \mathbf{x}_0, & u_i(0) &= u_{i0} \\ u_o(t) &= \mathbf{C}\mathbf{x}(t) + \mathbf{D}u_i(t), \end{aligned} \quad (14)$$

or, in the domain of Laplace transform (with zero initial conditions),

$$\begin{aligned} s\mathbf{T}_C \mathbf{X} &= \mathbf{G}\mathbf{X} + \mathbf{B}u_i \\ u_o &= \mathbf{C}\mathbf{X} + \mathbf{D}u_i \end{aligned} \quad (15)$$

in which  $\mathbf{X}$  is the Laplace transform of the vector  $\mathbf{x}$ . System (15) is the matrix description of the general structure of a voltage-mode OTA-C filter introduced in [1]. Thus, system (15) is a particular (linear) case of the general (nonlinear) system describing a filter circuit in Figure 1.

Turning back to the general case note that under assumption of invertibility of the matrix  $\mathbf{T}_C$ , Equation (10) can be reformulated as

$$\mathbf{x}'(t) = \begin{bmatrix} x'_1(t) \\ x'_2(t) \\ \vdots \\ x'_n(t) \end{bmatrix} = \mathbf{T}_C^{-1} \left( \begin{bmatrix} \sum_{l=1}^n G_{1l}(x_l(t)) \\ \sum_{l=1}^n G_{2l}(x_l(t)) \\ \vdots \\ \sum_{l=1}^n G_{nl}(x_l(t)) \end{bmatrix} + \begin{bmatrix} G_{b1}(u_i(t)) + C_{b1}u'_i(t) \\ G_{b2}(u_i(t)) + C_{b2}u'_i(t) \\ \vdots \\ G_{bn}(u_i(t)) + C_{bn}u'_i(t) \end{bmatrix} \right) \quad (16)$$

The above assumption is very natural. In particular, it is satisfied if every internal node of the filter has a grounded capacitor (this is the case for any canonical OTA-C structure). The problem of invertibility of matrix  $\mathbf{T}_C$  was thoroughly addressed in [1].

Denote the vector on the right-hand side of Equation (16) by  $f(u_i(t), \mathbf{x}(t))$ . Then, the differential system in question can be rewritten as

$$\mathbf{x}'(t) = f(u_i(t), \mathbf{x}(t)) \quad (17)$$

which, together with initial condition

$$\mathbf{x}(0) = \mathbf{x}_0, \quad u_i(0) = u_{i0} \quad (18)$$

is a classical Cauchy problem which can be easily solved numerically.

The above model can be applied to calculate nonlinear distortion of any OTA-C filter for any given input signal. For example, for input signal of the form  $u_i = U \cos(\omega t)$  we can, after solving Equations (17), (18), calculate harmonics in the output signal by evaluating the formula

$$h_n = \frac{2}{T} \left| \int_{-T/2}^{T/2} u_0(t) e^{-j2n\pi t/T} dt \right|, \quad n = 1, 2, \dots \quad (19)$$

where  $T$  is input signal period. Integral in Equation (19) can be evaluated numerically. This allows us to calculate, e.g. HD<sub>3</sub> and/or THD. In order to calculate other nonlinearity measures Equations (17), (18) has to be solved with different input excitation, e.g. to get IM3 we need two harmonic signals, and so on.

In order to handle system (17), (18) one needs to know transfer characteristics of all filter transconductors, i.e.  $G_{kl}$ ,  $G_{bk}$ ,  $G_{cl}$ ,  $G_d$  and  $G_o$ ,  $k, l = 1, 2, \dots, n$ , i.e. we need nonlinear macro-models of those transconductors. Transfer characteristic of a nonlinear transconductor can be simulated (or measured) as DC characteristics and then modelled using a power series expansion but in order to get better accuracy it is advisable to model transfer characteristic as a table of input voltages and corresponding output currents and apply interpolation for the point out of a table. In our implementation of the model we used spline interpolation [40]. Note that our analysis method can handle any kind of transconductor nonlinearity, because system (16) allows general transfer function  $G$ .

It should be emphasized that the method of evaluating nonlinear distortion described in this section is fast and efficient. Unlike the approaches based on Volterra series representation (e.g. [32–34]) or harmonic injection method [35], it is not restricted to handle weak nonlinearities only. Also, since the presented formalism is based on the OTA-C filter model in Figure 1, it is general enough to comprise all conceivable OTA-C filter structures. Matrix formulation makes the method easy to implement. Because there is one-to-one correspondence between the filter structure and the corresponding set of matrices, defining the filter and further manipulation (scaling) of its elements and even changing its structure is easy which makes the method useful for CAD and optimization (as demonstrated in Section 5).

### 3. NOISE ANALYSIS IN GENERAL OTA-C FILTERS

The literature contains several intuitive ideas on calculating noise, and attempts to solve noise problems for specific filters [36–39]. In contrast, this section provides complete, explicit, and easily evaluated formulas based on a general approach to noise analysis, and using matrix description as presented in Section 2, originally presented in [41]. We recall them here for the sake of completeness. These formulas can be applied to OTA-C filters with any known architecture and of any degree, and they can be easily implemented and used in computer-aided analysis/optimization software.

Assuming ideal, that is, lossless and, therefore, noiseless capacitors, the output noise of any OTA-C filter is a combination of the noise contributions of all its transconductors. As shown in Figure 3, the noise of a CMOS transconductor with value  $g_m$  can be described by an equivalent input-referred noise-voltage source,  $v_n$ , whose spectral density,  $S_n(f)$ , can be modelled as [36]

$$S_n(f) = \frac{S_t}{g_m} + \frac{S_f}{f} \quad (20)$$

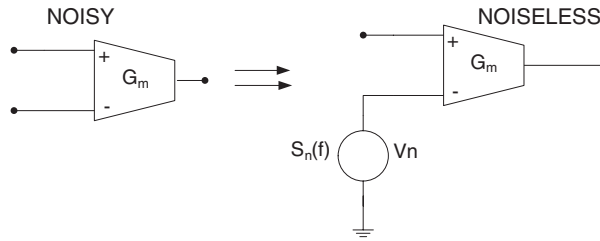


Figure 3. Representation of noise in an OTA by an equivalent input-voltage noise source.

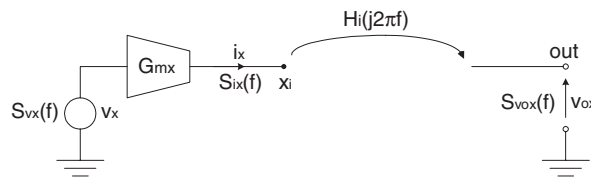


Figure 4. Noise contribution of an individual filter transconductor to the total output noise of the filter.

where the thermal noise component,  $S_t$ , and the flicker-noise component,  $S_f$ , depend on the transconductor topology and on biasing. We shall assume that noise sources associated with different OTAs are statistically independent.

To obtain the output- (and/or input-) noise spectrum of the general OTA-C topology in Figure 1 (for the purpose of noise evaluation we use the filter model in Figure 1 with transconductor values equal to linear transconductance of respective OTA, e.g.  $G_{m,ij} = dG_{ij}(v)/dv$  at  $v = 0$ ) explicitly, the noise contribution of each individual transconductor to the output (and/or input) noise must be determined. This can be modelled as shown in Figure 4. Let  $G_{mx}$  denote one of the filter transconductors (i.e.  $G_{m,bi}$ ,  $G_{m,ij}$ , etc.), which is connected to one of the nodes, say  $x_i$  (if the filter contains a non-trivial output summer then it has an additional-output-node, which will be denoted as  $x_0$ ). If the input-referred noise voltage of the noise source corresponding to  $G_{mx}$ , is labelled  $v_x$  with spectral density  $S_{v_x}(f)$ , the transconductor  $G_{mx}$  injects its noise current  $i_x = v_x G_{mx}$  into node  $x_i$ . The spectral density  $S_{i_x}(f)$  of this current is given by

$$S_{i_x}(f) = G_{mx}^2 S_{v_x}(f) \quad (21)$$

The corresponding output noise voltage  $v_{ox}$  can be calculated as

$$v_{ox} = i_x H_i = G_{mx} H_i v_x \quad (22)$$

where  $H_i$  is the current-to-voltage transimpedance from node  $x_i$  to the output of the filter. The corresponding spectral density  $S_{v_{ox}}(f)$  is given by

$$S_{v_{ox}}(f) = S_{i_x}(f) |H_i(j2\pi f)|^2 = G_{mx}^2 S_{v_x}(f) |H_i(j2\pi f)|^2 \quad (23)$$

Using Equation (15), it is easy to show that the transfer functions  $H_j(s)$ ,  $j = 1, 2, \dots, n$  are components of the  $1 \times n$  vector  $\mathbf{H}_{cv}$  defined as

$$\mathbf{H}_{cv}(s) = \mathbf{C}(s\mathbf{T}_C - \mathbf{G})^{-1} \tag{24}$$

If a non-trivial output summer is present (cf. Figure 1) we need also the current-to-voltage transfer function

$$H_0 = G_{mo}^{-1} \tag{25}$$

from the output node to itself. Thus, each filter transconductor injects its noise current with spectral density (21) into one of the internal nodes of the filter (or directly into the output node if the filter has a non-trivial output summer). This current is then converted into the output noise voltage according to (23). To calculate the total output noise voltage of the filter we add all the corresponding noise spectra. In general, the outputs of one input transconductor  $G_{m.bi}$ , and  $n$  transconductors  $G_{m.ij}$ ,  $j = 1, \dots, n$ , are connected to each internal node  $x_i$ . In the presence of a non-trivial output summer we have an additional output node,  $x_0$ , with outputs of transconductors  $G_{m.cj}$ ,  $j = 1, \dots, n$ ,  $G_{md}$ , and  $G_{mo}$ . Let us define the auxiliary matrices

$$\begin{aligned} \mathbf{S}_t &= [S_{t.ij}]_{i,j=1}^n, & \mathbf{S}_f &= [S_{f.ij}]_{i,j=1}^n, & \mathbf{S}_{tb} &= [S_{tb.1} \dots S_{tb.n}]^T, & \mathbf{S}_{fb} &= [S_{fb.1} \dots S_{fb.n}]^T \\ \mathbf{S}_{tc} &= [S_{tc.1} \dots S_{tc.n}], & \mathbf{S}_{fc} &= [S_{fc.1} \dots S_{fc.n}] \\ \mathbf{S}_{td} &= S_{td}, & \mathbf{S}_{fd} &= S_{fd}, & \mathbf{S}_{to} &= S_{to}, & \mathbf{S}_{fo} &= S_{fo} \end{aligned} \tag{26}$$

representing the thermal noise (subscript t) and flicker noise (subscript f) of transconductors  $G_{m.ij}$ ,  $G_{m.bi}$ ,  $G_{m.ci}$ ,  $G_{md}$ , and  $G_{mo}$ , respectively. Let us denote by  $\overline{\mathbf{A}}$  component-by-component modulus of matrix  $\mathbf{A}$  (i.e. if  $\mathbf{A} = [a_{ij}]_{i,j=1}^n$  then  $\overline{\mathbf{A}} = [|a_{ij}|]_{i,j=1}^n$ ).<sup>‡</sup> Denote further by ‘ $\circ$ ’ the Hadamard product of two matrices, i.e. if  $\mathbf{P} = [p_{ij}]_{i,j=1}^n$  and  $\mathbf{Q} = [q_{ij}]_{i,j=1}^n$ , we have  $\mathbf{P} \circ \mathbf{Q} = [p_{ij}q_{ij}]_{i,j=1}^n$ ,<sup>‡</sup> and let  $\hat{\mathbf{I}} = [1 \dots 1]^T$  be an  $n \times 1$  vector. Define the function  $F(\mathbf{P}, \mathbf{Q}, \mathbf{R})(x)$  as

$$F(\mathbf{P}, \mathbf{Q}, \mathbf{R})(x) = \mathbf{P} \circ [\mathbf{Q} + (2\pi/x)\mathbf{P} \circ \mathbf{R}] \tag{27}$$

where  $\mathbf{P}$ ,  $\mathbf{Q}$ , and  $\mathbf{R}$  are matrices of the same dimension and  $x$  is a real variable. It follows from (20) and (21) that the spectral densities,  $S_i(\omega)$ , of the total noise current injected into the nodes  $x_i$ ,  $i = 1, \dots, n$ , can be expressed, using (27), as components of the current spectral-density vector  $\mathbf{S}$ , given by

$$\mathbf{S}(\omega) = [S_1(\omega) \dots S_n(\omega)]^T = F(\overline{\mathbf{G}}, \mathbf{S}_t, \mathbf{S}_f)(\omega) \cdot \hat{\mathbf{I}} + F(\overline{\mathbf{B}}, \mathbf{S}_{tb}, \mathbf{S}_{fb})(\omega) \tag{28}$$

Analogously, if there is a non-trivial output summer, the spectral density  $S_0(\omega)$  of the noise current injected into node  $x_0$  is given by

$$S_0(\omega) = F(\overline{\mathbf{C}}, \mathbf{S}_{tc}, \mathbf{S}_{fc})(\omega) \cdot \hat{\mathbf{I}} + F(\overline{\mathbf{D}}, \mathbf{S}_{td}, \mathbf{S}_{fd})(\omega) + F(\overline{\mathbf{O}}, \mathbf{S}_{to}, \mathbf{S}_{fo})(\omega) \tag{29}$$

<sup>‡</sup>The same definition holds, with obvious changes, for  $n \times 1$ ,  $1 \times n$ , and  $1 \times 1$  matrices.

The spectral density  $S_{no}(\omega)$  of the total output-noise voltage  $v_{no}$  can then be calculated as

$$S_{no}(\omega) = |\mathbf{H}_{cv}(\omega)|^2 \mathbf{S}(\omega) + H_0^2 S_0(\omega) \quad (30)$$

where  $|\mathbf{H}_{cv}(\omega)|^2 = \mathbf{H}_{cv}(j\omega) \circ \mathbf{H}_{cv}(-j\omega)$ , with  $\mathbf{H}_{cv}$  and  $H_0$  given by Equations (24) and (25), respectively. Equation (30) permits the output-noise spectrum of any OTA-C filter to be calculated; the output-noise voltage is then obtained by integrating Equation (30) over a suitable frequency range. The equivalent input-noise spectrum  $S_{ni}(\omega)$  can be obtained by dividing Equation (30) by the squared magnitude of a filter's transfer function (from Equation (15) we have  $H(s) = \mathbf{C}(s\mathbf{T}_C - \mathbf{G})\mathbf{B} + \mathbf{D}$ ) [41]. It is worth noting that the matrix formulation makes implementing the presented expressions in a computer program particularly convenient, which permits the noise analysis of arbitrary OTA-C filters to be carried out automatically.

In practice, frequently all filter transconductors are identical, that is,  $S_{t,ij} = S_t$ ,  $S_{f,ij} = S_f$ ,  $i, j = 1, \dots, n$ ,  $S_{tb,i} = S_{tc,i} = S_t$ ,  $S_{fb,i} = S_{fc,i} = S_f$ ,  $i = 1, \dots, n$ ,  $S_{td} = S_{to} = S_t$ ,  $S_{fd} = S_{fo} = S_f$  (cf. (26)), where  $S_t$  and  $S_f$  are the noise parameters of the transconductors. Then, Equations (28) and (29) take the form

$$\mathbf{S}(\omega) = (\overline{\mathbf{G}\hat{\mathbf{I}} + \overline{\mathbf{B}}})S_t + \frac{2\pi}{\omega}(\overline{\mathbf{G}} \circ \overline{\mathbf{G}\hat{\mathbf{I}}} + \overline{\mathbf{B}} \circ \overline{\mathbf{B}})S_f \quad (31)$$

$$S_0(\omega) = (\overline{\mathbf{C}\hat{\mathbf{I}} + \overline{\mathbf{D}} + \overline{\mathbf{O}}})S_t + \frac{2\pi}{\omega}(\overline{\mathbf{C}} \circ \overline{\mathbf{C}\hat{\mathbf{I}}} + \overline{\mathbf{D}} \circ \overline{\mathbf{D}} + \overline{\mathbf{O}} \circ \overline{\mathbf{O}})S_f \quad (32)$$

#### 4. VERIFICATION OF THE NONLINEARITY AND NOISE ANALYSIS TOOLS

In order to verify the accuracy of the proposed approach, comparisons between theoretical results and SPICE simulations have been carried out. The numerical results have been obtained using 4th order Adams–Bashforth's [40] method to integrate differential equation (17) and three-point composite Newton–Cotes quadrature [40] to calculate coefficients  $C_n$  in (19) (Figure 4).

For the first comparison we use a simple differential-pair transconductor shown in Figure 5. The circuit was implemented in standard 0.35  $\mu\text{m}$  AMS technology and simulated using SPICE. The OTA macromodel parameters extracted from the simulations are:  $i_{out}(v_{id}) = g_m v_{id} + g_{m3}(v_{id})^3 + g_{m5}(v_{id})^5 = 10^{-4}v_{id} - 4.2 \times 10^{-5}(v_{id})^3 - 3.4 \times 10^{-5}(v_{id})^5$  ( $\mu\text{A}$ ) ( $v_{id}$  in volts; accuracy of the series better than 0.1% for  $v_{id} < 0.75$  V); transconductance  $g_m = 100 \mu\text{A/V}$ ; noise parameters (20):  $S_t = 5.2 \times 10^{-16}$  V A/Hz,  $S_f = 2.3 \times 10^{-10}$  V<sup>2</sup>.

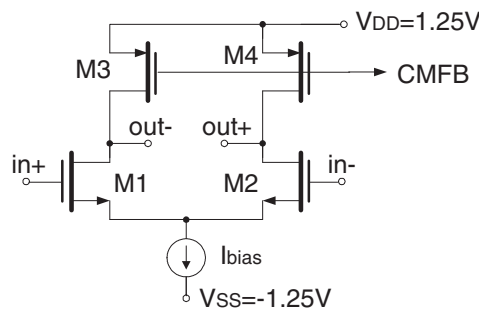


Figure 5. Simple differential-pair transconductor (common-mode feedback circuit not shown).

The OTA circuit in Figure 5 was used to implement the 3rd order Butterworth low-pass filter in a leap-frog (LF) structure shown in Figure 6 (actual filter was implemented in fully differential structure). The element values are:  $C_1 = 2.37$  pF,  $C_2 = 2.11$  pF,  $C_3 = 0.79$  pF; the OTAs in Figure 5 were used as active elements of the filter. Three dB frequency of the filter is 10 MHz. Figures 7–9 show THD *versus* frequency with 0.3 V input signal amplitude, THD *versus* input signal amplitude for 5 MHz input frequency, and output noise spectrum *versus* frequency, respectively. The agreement between theoretical results (line) and SPICE simulation results (point) is very good. It should be emphasized that transient analysis performed by integrating Equation (17) is, due to OTA macromodelling, about three orders of magnitude faster than the one carried out with transistor level simulation using SPICE.

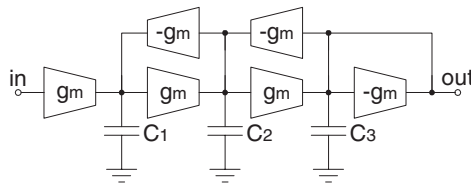


Figure 6. Diagram of 3rd order LF filter.

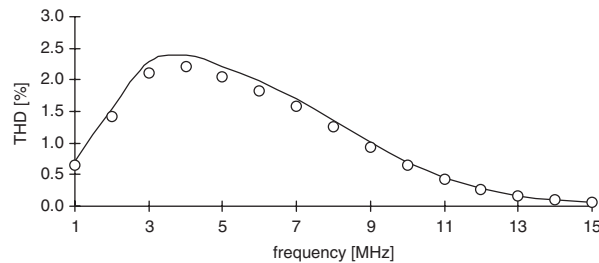


Figure 7. THD *versus* frequency for filter in Figure 6 with 0.3 V input amplitude: theoretical data (line), and simulation (points).

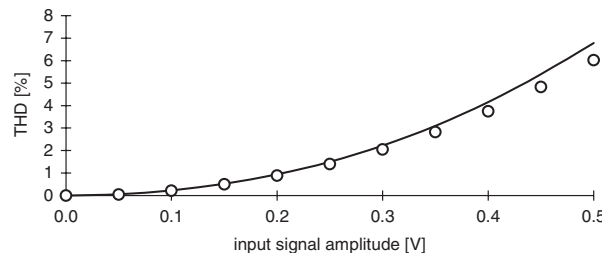


Figure 8. THD *versus* input signal amplitude for filter in Figure 6 with 5 MHz sine wave: theoretical data (line), and simulation (points).

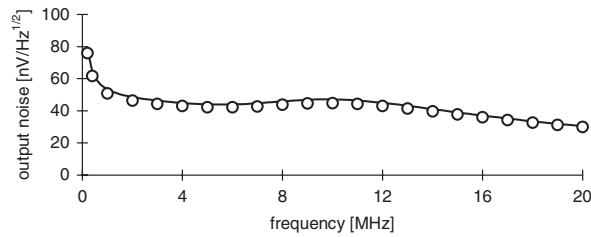


Figure 9. Output noise spectrum *versus* frequency for filter in Figure 6: theoretical data (line) and simulation (points).

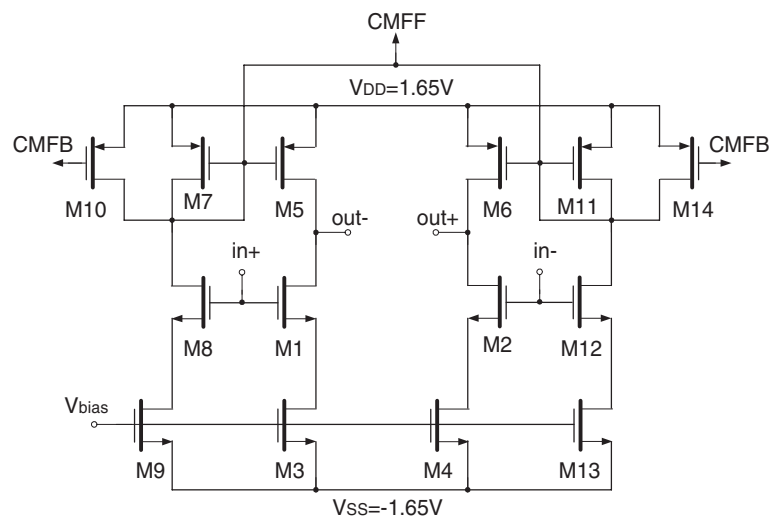


Figure 10. Linearized OTA circuit [42].

To validate the approach more intensively, comparisons between the theoretical, SPICE simulations and also experimental measurements have been carried out. For this a more linear OTA [42] was designed and fabricated using AMI 0.5  $\mu\text{m}$  technological process. The OTA macromodel parameters are extracted from the simulations similar to the previous example. The transconductance of a single OTA was designed to be equal to  $g_m = 345 \mu\text{A/V}$ ; noise parameters:  $S_t = 8.17 \times 10^{-20} \text{ V A/Hz}$ ,  $S_f = 0$  (flicker noise components are negligible). OTA nonlinearity was represented, for the purpose of solving Equation (17), by spline interpolation of its tabularized transfer function.

The OTA circuit of Figure 10 was used to implement a 5th order Bessel low-pass filter. The 3 dB frequency of the filter is 10 MHz. The filter can be realized in one of 50 different structures—both multiple-loop feedback (including leap-frog (LF) and IFLF) and cascade realizations. Using the approach described in Section 2, the analysis of all filter structures for best THD performance for a 0.5  $V_{pp}$  at 10 MHz has been carried out. According to this analysis, the cascade structure with

two biquads followed by a first order block (Figure 11) turned out to be the best (THD = -61 dB) (for comparison, LF structure has THD = -58.4 dB, the worst structure of the considered has THD = -56.2 dB), and this structure was designed and fabricated. The capacitor element values are:  $C_1 = 2.79$  pF,  $C_2 = 2.34$  pF,  $C_3 = 5.11$  pF,  $C_4 = 1.625$  pF,  $C_5 = 2.98$  pF, power supply equal to  $\pm 1.65$  V. The chip micro-photograph of the filter structure is shown in Figure 12.

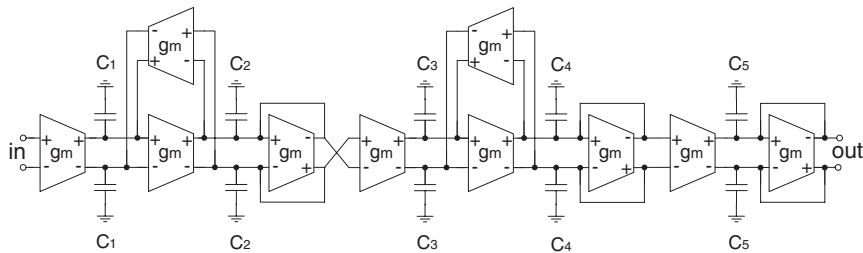


Figure 11. Block diagram of 5th order Bessel filter-cascade structure (2:2:1).

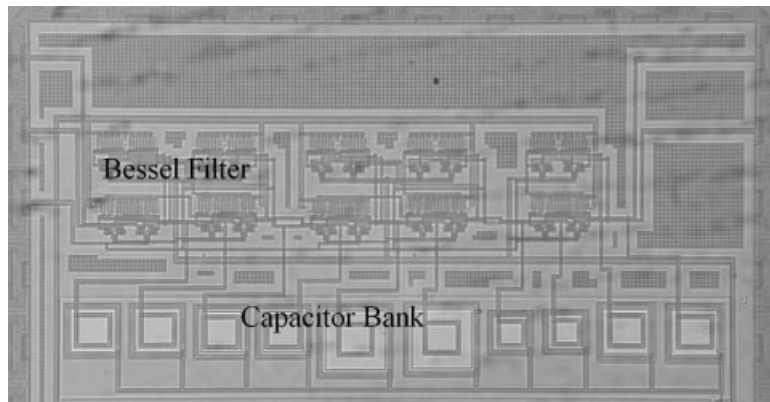


Figure 12. Micro-photograph of the filter in Figure 11.

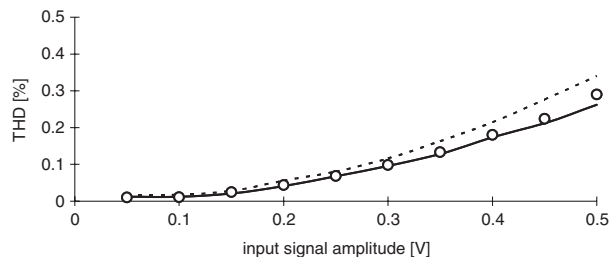


Figure 13. THD versus input signal amplitude for filter in Figure 11 at 10 MHz: theoretical data (solid line), SPICE simulation (points), and experimental measurements (dashed line).

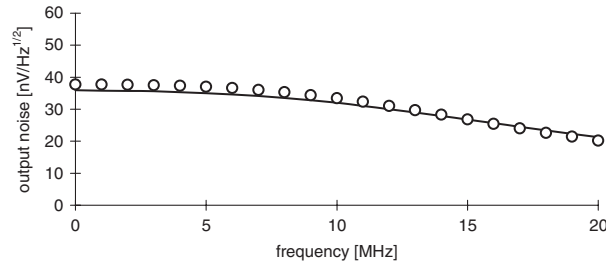


Figure 14. Output noise spectrum *versus* frequency for filter in Figure 11: theoretical data (solid line) and spice simulation (points).

Figures 13 and 14 show THD *versus* input signal amplitude at 10 MHz and output noise spectrum *versus* frequency, respectively. The agreement between theoretical results SPICE simulation results and experimental measurement results is very good. These results verify the approach and models proposed in Sections 2 and 3.

## 5. PERFORMANCE OPTIMIZATION OF OTA-C FILTERS

The nonlinear distortion and noise evaluation tools presented in Sections 2 and 3 are well suited to be used in CAD and optimization of OTA-C filters. The optimization methodology, which takes advantage of the matrix description of the OTA-C filter model in Figure 1, is the following. Let  $\mathbf{P}$  and  $\mathbf{Q}$  be two diagonal  $n \times n$  matrices with positive elements, i.e.

$$\mathbf{P} = \text{diag}\{p_1, \dots, p_n\}, \quad \mathbf{Q} = \text{diag}\{q_1, \dots, q_n\} \quad (33)$$

We also assume that the matrix  $\mathbf{T}$  is diagonal (i.e. the filter contains only grounded capacitors). Then the transfer function formula (linear case) can be rewritten as

$$\begin{aligned} H(s) &= \mathbf{C}(s\mathbf{T} - \mathbf{G})^{-1}\mathbf{B} + \mathbf{D} = \mathbf{C}\mathbf{P}\mathbf{P}^{-1}(s\mathbf{T} - \mathbf{G})^{-1}\mathbf{Q}^{-1}\mathbf{Q}\mathbf{B} + \mathbf{D} \\ &= \mathbf{C}\mathbf{P}(s\mathbf{Q}\mathbf{T}\mathbf{P} - \mathbf{Q}\mathbf{G}\mathbf{P})^{-1}\mathbf{Q}\mathbf{B} + \mathbf{D} \end{aligned} \quad (34)$$

Let us define the following matrices:

$$\hat{\mathbf{T}} = \mathbf{Q}\mathbf{T}\mathbf{P}, \quad \hat{\mathbf{G}} = \mathbf{Q}\mathbf{G}\mathbf{P}, \quad \hat{\mathbf{C}} = \mathbf{C}\mathbf{P}, \quad \hat{\mathbf{B}} = \mathbf{Q}\mathbf{B}, \quad \hat{\mathbf{D}} = \mathbf{D} \quad (35)$$

It is seen from (34) that the equivalence transformation (35) leads to the matrices  $\hat{\mathbf{T}}$ ,  $\hat{\mathbf{G}}$ ,  $\hat{\mathbf{C}}$ ,  $\hat{\mathbf{B}}$  and  $\hat{\mathbf{D}}$ , and define a new filter, which has the same topology and transfer function but different (re-scaled) element values, and, usually, different performance parameters.

Note also that  $\mathbf{Q}$ ,  $\mathbf{P}$  and  $\mathbf{T}$  need not be diagonal, however, they cannot be arbitrary invertible matrices as well, because matrix  $\hat{\mathbf{T}}$  obtained as a result of transformation (35) has to be symmetric, positively definite with positive diagonal and non-positive non-diagonal entries in order to define an OTA-C filter (see [1] for details). In particular, if  $\mathbf{P}$  and  $\mathbf{Q}$  are diagonal but  $\mathbf{T}$  is general then matrices  $\mathbf{P}$  and  $\mathbf{Q}$  have to satisfy the condition  $p_i q_j = p_j q_i$  whenever  $i \neq j$  and  $\mathbf{T}_{ij} \neq 0$ . For

diagonal  $\mathbf{T}$ , i.e. for the filter with only grounded capacitors the above condition is satisfied automatically so  $\mathbf{P}$  and  $\mathbf{Q}$  are independent.

The task is now to find the matrices  $\mathbf{P}$  and  $\mathbf{Q}$  so that the filter performance parameter(s) of interest is(are) optimized. Thus, we came up with a clear optimization procedure:

1. Take an initial realization of the transfer function  $H(s)$  given by the set of matrices  $\mathbf{T}$ ,  $\mathbf{G}$ ,  $\mathbf{B}$ ,  $\mathbf{C}$  and  $\mathbf{D}$ .
2. Use the matrix elements of  $\mathbf{P}$  and  $\mathbf{Q}$ , i.e.  $p_1, \dots, p_n, q_1, \dots, q_n$ , as optimization variables and optimize the target function  $F = F(\mathbf{T}, \mathbf{G}, \mathbf{B}, \mathbf{C}, \mathbf{D}; \mathbf{P}, \mathbf{Q})$ , which may be dynamic range, integrated noise, THD, etc.

Usually, we have some design constraints such as the maximum value of total capacitance of the filter, maximum power consumption of the filter which depends on transconductance value, allowable capacitance ratio, i.e. the ratio of maximum to minimum capacitance values in the filter, and so on. Some or all of these constraints have to be taken into account in the optimization process. In general, constraints can be written as follows:

$$m_j \leq c_j(\mathbf{T}, \mathbf{G}, \mathbf{B}, \mathbf{C}, \mathbf{D}; \mathbf{P}, \mathbf{Q}) \leq M_j, \quad j = 1, \dots, N_c \quad (36)$$

where  $N_c$  is the number of constraints,  $c_j$  is the  $j$  constraint function (e.g. total capacitance of the filter) which is dependent on matrices describing the filter and optimization variables, while  $m_j$  and  $M_j$  are minimum and maximum values of  $c_j$  (which may be finite or infinite).

The optimization itself can be carried out using any available numerical procedure embedded into the optimization system. Choice of the optimization procedure depends on the complexity of the problem and constraints.

For the rest of this section we discuss a representative example: performance optimization of OTA-C filters in cascade realization. The problem is to find the optimal pole-zero pairing, optimal cascading sequence, and optimal gain distribution so that the parameter of interest is optimized. There is a rich literature (e.g. [43, 44]) discussing that problem and its solutions (usually quite complex procedures which are impracticable for high-order filters, or just rules of thumb) in more or less general setting and usually for some specific performance parameters. In practice, the only way to find truly optimal solution of the general problem is exhaustive search through all possible cascade sequencing and performing parameter optimization for each of them. Fortunately, by using the procedures described in the previous sections we can afford it because these tools are very fast.

For the sake of illustration we shall consider performance optimization of 8th order Butterworth filter in cascade realization (Figure 15) with biquads shown in Figure 16. In the optimization process we assume two degrees of freedom. The first one is biquad sequencing (which is equivalent to pole-zero pairing for Butterworth filter is an all-pole one). The second are biquad gains, which will be denoted as  $K_i, i = 1, 2, 3, 4$ . Gains are adjusted by changing transconductance  $g_b$  of input transconductor; the value of transconductance  $g_m = 100 \mu\text{A}/\text{V}$  is fixed;  $g_b \in [70.7 \mu\text{A}/\text{V}, 141.4 \mu\text{A}/\text{V}]$ ,



Figure 15. Block diagram of 8th order cascade filter.

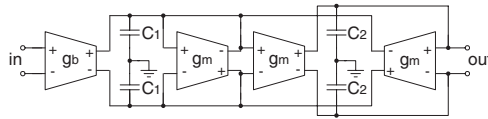


Figure 16. Fully differential biquad used in the filter in Figure 15.

which allows us to change  $K_i$  in the range  $[2^{-1/2}, 2^{1/2}]$  ( $[-3 \text{ dB}, +3 \text{ dB}]$ ). We assumed unity gain setting for the whole filter, i.e.  $(K_1 + K_2 + K_3 + K_4 = 0 \text{ dB})$ .

In terms of the general OTA-C filter model, the matrices corresponding to the filter in Figure 15 are

$$\mathbf{G} = \begin{bmatrix} \mathbf{G}_1 & \mathbf{0}_2 & \mathbf{0}_2 & \mathbf{0}_2 \\ \mathbf{G}_2 & \mathbf{G}_1 & \mathbf{0}_2 & \mathbf{0}_2 \\ \mathbf{0}_2 & \mathbf{G}_2 & \mathbf{G}_1 & \mathbf{0}_2 \\ \mathbf{0}_2 & \mathbf{0}_2 & \mathbf{G}_2 & \mathbf{G}_1 \end{bmatrix} \quad (37)$$

with

$$\mathbf{G}_1 = \begin{bmatrix} -g_m & -g_m \\ g_m & 0 \end{bmatrix}, \quad \mathbf{G}_2 = \begin{bmatrix} 0 & g_m \\ 0 & 0 \end{bmatrix}, \quad \mathbf{0}_2 = 2 \times 2 \text{ zero matrix} \quad (38)$$

and

$$\mathbf{T} = \text{diag}\{C_{11}, C_{12}, C_{21}, C_{22}, C_{31}, C_{32}, C_{41}, C_{42}\} \quad (39)$$

$$\mathbf{B} = [g_m \ 0 \ \dots \ 0]^T, \quad \mathbf{C} = [0 \ \dots \ 0 \ 1], \quad \mathbf{D} = 0$$

where the first index of elements of matrix  $\mathbf{T}$  refers to the biquad number (e.g.  $C_{i1}$  is  $C_1$  in biquad  $H_i$  and so on). We assume that initial value of input transconductance  $g_b$  is equal to  $g_m$  for each biquad. Setting gains as above is equivalent to using the transforms (35) with  $\mathbf{P}$ ,  $\mathbf{Q}$  as in (33) with  $q_1 = q_2 = K_1$ ,  $q_3 = q_4 = K_1 K_2$ ,  $q_5 = q_6 = K_1 K_2 K_3$ ,  $q_7 = q_8 = 1$ , and  $p_i = 1/q_i$ ,  $i = 1, \dots, 8$ . Thus, we actually have a constrained optimization problem with three independent variables.

Permutation of filter blocks is realized by permutation of corresponding elements of the matrix  $\mathbf{T}$ . Original block sequencing: 1234 corresponds to original location of elements, i.e.  $\{C_{11}, C_{12}, C_{21}, C_{22}, C_{31}, C_{32}, C_{41}, C_{42}\}$ . Any other permutation, e.g.  $klpq$  is given by  $\{C_{k1}, C_{k2}, C_{l1}, C_{l2}, C_{p1}, C_{p2}, C_{q1}, C_{q2}\}$ .

We consider three variants of the filter: variant I with differential pair transconductors (Figure 5) implemented in standard  $0.35 \mu\text{m}$  CMOS process, variant II with linearized OTAs [45] (Figure 17) implemented in  $0.5 \mu\text{m}$  technology, and variant III with linearized OTAs [42] (Figure 10) implemented in  $0.35 \mu\text{m}$ . The 3dB cutoff frequency of the filter equals 8 MHz for all variants. Capacitance values are:  $C_{11} = 0.51 \text{ pF}$ ,  $C_{12} = 1.96 \text{ pF}$ ,  $C_{21} = 0.60 \text{ pF}$ ,  $C_{22} = 1.66 \text{ pF}$ ,  $C_{31} = 0.90 \text{ pF}$ ,  $C_{32} = 1.11 \text{ pF}$ ,  $C_{41} = 2.56 \text{ pF}$ ,  $C_{42} = 0.39 \text{ pF}$ , power supply equal to  $\pm 1.65 \text{ V}$ .

Optimization was carried out using the software written in C, implementing both nonlinearity and noise evaluation procedures of Sections 2 and 3, and numerical optimization routines. OTA



Table II. Optimization results for the filter in Figure 15—Variant I (values in brackets refer to CADENCE simulation results).

Target parameter	Optimal configuration						
	Biquad sequence	Biquad gains (dB)				Target parameter value	Improvement over reference (dB)
		$K_1$	$K_2$	$K_3$	$K_4$		
Noise	$H_3H_4H_2H_1$	3.0	3.0	-3.0	-3.0	169 [172] $\mu$ V	8.2 [8.1]
THD	$H_3H_1H_2H_4$	-3.0	-2.1	2.1	3.0	-37.7 [-38] dB	6.2 [5.6]
DR	$H_4H_3H_2H_1$	1.8	-1.4	-0.9	0.5	47.4 [47.5] dB	6.7 [6.4]

Table III. Optimization results for the filter in Figure 15—Variant II [45] (values in brackets refer to CADENCE simulation results).

Target parameter	Optimal configuration						
	Biquad sequence	Biquad gains (dB)				Target parameter value	Improvement over reference (dB)
		$K_1$	$K_2$	$K_3$	$K_4$		
Noise	$H_3H_4H_2H_1$	3.0	3.0	-3.0	-3.0	458 [533] $\mu$ V	8.1 [6.1]
THD	$H_3H_1H_2H_4$	-1.7	-1.3	0.0	3.0	-54.8 [-53.3] dB	8.3 [6.9]
DR	$H_4H_3H_2H_1$	2.4	-1.5	-1.0	0.1	48.9 [48.4] dB	6.6 [5.5]

Table IV. Optimization results for the filter in Figure 15—Variant III [42] (values in brackets refer to CADENCE simulation results).

Target parameter	Optimal configuration						
	Biquad sequence	Biquad gains (dB)				Target parameter value	Improvement over reference (dB)
		$K_1$	$K_2$	$K_3$	$K_4$		
Noise	$H_3H_4H_2H_1$	3.0	3.0	-3.0	-3.0	275 [342] $\mu$ V	8.2 [5.8]
THD	$H_3H_2H_1H_4$	-1.7	-1.3	0.0	3.0	-60.5 [-59.8] dB	3.7 [2.0]
DR	$H_4H_3H_2H_1$	1.3	-1.1	-0.6	0.4	56.5 [56.0] dB	6.6 [5.0]

be emphasized that the optimization process including exhaustive search through all 24 biquad permutations and numerical optimization of target function involving multiple THD evaluations (note that in case of DR it is necessary to perform nested nonlinear optimization in order to find input signal level corresponding to required THD value) is fully automated and very fast. For example, transient analysis of the filter in Figure 15 using OTA macromodelling and integration of Equation (17) involves less than 0.04 s of CPU time regardless filter variant *versus* 16.2 s (variant I), 17.2 s (variant II), and 19 s (variant III) for transistor-level simulation, with almost no loss of accuracy.

## 6. CONCLUSIONS

Efficient procedures for evaluating nonlinear distortion and noise valid for any OTA-C filter of arbitrary order are developed based on matrix description of a general OTA-C filter model. In particular, a general description of OTA-C filters with nonlinear transconductors is introduced. The presented method allows carrying out an effective and fast transient analysis of any OTA-C filter using standard numerical methods and can be applied to determine the THD or other nonlinearity measures of filters containing nonlinear transconductors. On the other hand, universal expressions are derived that permit computing the filter noise. The model and all the formulas are implemented in a software package that allows calculating OTA-C filter nonlinearity, noise and dynamic range. Efficiency and accuracy of the approach is shown by comparing the results obtained using the theoretical models with simulation and experimental data. As an application, we implement a simple optimization procedure that utilizes our analysis methods and use it to find optimal block sequencing and gain distribution for 8th order Butterworth filter in cascade realization.

## REFERENCES

1. Koziel S, Szczepanski S, Schaumann R. General approach to continuous-time  $G_m$ -C filters. *International Journal of Circuit Theory and Applications* 2003; **31**:361–383.
2. Tsvividis YP. Integrated continuous-time filter design—an overview. *IEEE Journal of Solid-State Circuits* 1994; **29**:166–176.
3. Bowron P, Mezher KA, Muhieddine AA. Complete dynamic range for second-order analogue active filters. *Proceedings of the IEEE International Symposium on Circuits and Systems*, vol. 2, San Diego, CA, 10–13 May 1992; 847–850.
4. Bowron P, Mezher KA, Muhieddine AA. The dynamic range of second-order continuous-time active filters. *IEEE Transactions on Circuits and Systems I* 1996; **43**(5):370–373.
5. Shi CJR, Tan X-D. Canonical symbolic analysis of large analog circuits with determinant decision diagram. *IEEE Transactions on Computer-Aided Design of Integrated Circuits and Systems* 2000; **19**:1–18.
6. Mayaram K, Lee DC, Moinian S, Rich DA, Roychowdhury J. Computer-aided circuit analysis tools for RFIC simulation: algorithms, features and limitations. *IEEE Transactions on Circuits and Systems—II, Analog and Digital Signal Processing* 2000; **47**(4):274–285.
7. Ray BN, Chaudhuri PP, Nandi PK. Efficient synthesis of OTA network for linear analog functions. *IEEE Transactions on Computer-Aided Design of Integrated Circuits and Systems* 2002; **21**(5):517–533.
8. Pai PKD, Abidi AA. A 40-mW 55 Mb/s CMOS equalizer for use in magnetic storage read channels. *IEEE Journal of Solid-State Circuits* 1994; **29**:489–499.
9. Khorramabadi H, Tarsie MJ, Woo NS. Baseband filters for IS-95 CDMA receiver applications featuring digital automatic frequency tuning. *International Solid State Circuits Conference*, San Francisco, 1996; 172–173.
10. Dehaene W, Steyaert MSJ, Sansen W. A 50-MHz standard CMOS pulse equalizer for hard disk read channels. *IEEE Journal of Solid-State Circuits* 1997; **32**:977–988.
11. Hassan A, Sharaf K, El-Ghitani H, Ragai HF. The design and implementation of a bandpass Gm-C filter for bluetooth. *Proceedings of the Midwest Symposium on Circuits and Systems (MWSCAS)*, Stillwater, OK, USA, vol. 2, 2002; 629–632.
12. Mehrmanesh S, Atarodi M. A high dynamic range CMOS variable gain filter for ADSL. *Proceedings of the International Symposium on Circuits and Systems (ISCAS)*, Scottsdale, Arizona, USA, vol. 4, 2002; 257–260.
13. Schaumann R, Ghausi MS, Laker KR. *Design of Analog Filters, Passive, Active RC, and Switched Capacitor*. Prentice-Hall: Englewood Cliffs, NJ, 1990.
14. Deliyannis T, Sun Y, Fidler JK. *Continuous-Time Active Filter Design*. CRC Press: Boca Raton, FL, U.S.A., 1999.
15. Geiger RL, Sánchez-Sinencio E. Active filter design using operational transconductance amplifiers: a tutorial. *IEEE Circuit and Devices Magazine* 1985; **1**:20–32.
16. Nauta B. *Analog CMOS Filters for Very High Frequencies*. Kluwer Academic Publishers: Dordrecht, 1993.

17. Sun Y (ed.). *Design of High Frequency Integrated Analogue Filters*. The Institution of Electrical Engineers: London, 2002.
18. Sánchez-Sinencio E, Silva-Martinez J. CMOS transconductance amplifiers, architectures and active filters: a tutorial. *IEE Proceedings—Circuits Devices and Systems* 2000; **147**(1):3–12.
19. Hayahara E, Enomoto M. Deriving technique of equivalent forms from general filter circuits and application. *IEEE Transactions on Circuits and Systems—I: Fundamental Theory and Applications* 1999; **46**(9):1037–1041.
20. Sun Y, Fidler JK. Synthesis and performance analysis of universal minimum component integrator-based IFLF OTA-grounded capacitor filter. *IEE Proceedings—Circuits Devices and Systems* 1996; **143**(2):107–114.
21. Koziel S, Szczepanski S. Structure generation and performance comparison of canonical elliptic  $G_m$ -C filters. *Proceedings of the International Conference on Electronic Circuits and Systems (ICECS)*, vol. I, Dubrovnik, Croatia, 2002; 157–160.
22. Mehrmanesh S, Aslanzadeh HA, Vahidfar MB, Atarodi M. A 1.8 V high dynamic range CMOS  $G_m$ -C filter for portable video systems. *Proceedings of the International Conference on Microelectronics (ICM)*, Beirut, Lebanon 2002; 38–41.
23. Jendernalik W, Szczepanski S. A CMOS OTA-C channel-select filter for mobile receiver. *Proceedings of the International Conference on Circuits and System Communication (ICCSC)*, St. Petersburg, Russia, 2002; 50–53.
24. Salthouse CD, Sarpeshkar R. A practical micropower programmable bandpass filter for use in bionic ears. *IEEE Journal of Solid-State Circuits* 2003; **38**(1):63–70.
25. Emira AA, Sanchez-Sinencio E. A pseudo differential complex filter for bluetooth with frequency tuning. *IEEE Transactions on Circuits and Systems II* 2003; **50**(10):742–754.
26. D'Amico S, Baschiroto A. 0.18- $\mu$ m CMOS  $G_m$ -C digitally tuned filter for telecom receivers. *Proceedings of the International Symposium on Circuits and Systems (ISCAS)*, Vancouver, Canada, vol. 1, 2003; 493–496.
27. Shin J, Min S, Kim S, Choi J, Lee S, Park H, Kim J. 3.3-V baseband  $G_m$ -C filters for wireless transceiver applications. *Proceedings of the International Symposium on Circuits and Systems (ISCAS)*, Vancouver, Canada, vol. 1, 2003; 457–460.
28. Mehrmanesh S, Vahidfar MB, Aslanzadeh HA, Atarodi M. An ultra low-voltage  $G_m$ -C filter for video applications. *Proceedings of the International Symposium on Circuits and Systems (ISCAS)*, Vancouver, Canada, vol. 1, 2003; 561–564.
29. Palaskas Y, Tsvividis Y. Dynamic range optimization of weakly nonlinear, fully balanced,  $G_m$ -C filters with power dissipation constraints. *IEEE Transactions on Circuits and Systems—II* 2003; **50**(10):714–727.
30. Roberts GW, Sedra AS. A general class of current amplifier-based biquadratic filter circuits. *IEEE Transactions on Circuits and Systems—I* 1992; **38**:257–263.
31. Koziel S, Szczepanski S. Dynamic range comparison of voltage-mode and current-mode state-space  $G_m$ -C biquad filters in reciprocal structures. *IEEE Transactions on Circuits and Systems—I* 2003; **50**(10):1245–1255.
32. Szczepanski S, Schaumann R. Nonlinearity induced distortion of the transfer function shape in high-order OTA-C filters. *Analog Integrated Circuits and Signal Processing* 1992; **3**:143–151.
33. Liang ZQ, Billings SA. Evaluation of output frequency responses of nonlinear systems under multiple inputs. *IEEE Transactions on Circuits and Systems—II* 2000; **47**:28–38.
34. Wambacq P, Sansen W. *Distortion Analysis of Analog Integrated Circuits*. Kluwer Academic Publishers: Dordrecht, 1998.
35. Mahattanakul J, Bunyakate C. Harmonic injection method: a novel method for harmonic distortion analysis. *Proceedings of the International Symposium on Circuits and Systems (ISCAS)*, Sydney, Australia, vol. 3, 2001; 85–88.
36. Brambilla A, Espinosa G, Montecchi F, Sánchez-Sinencio E. Noise optimization in operational transconductance amplifier filters. *Proceedings of the International Symposium on Circuits and Systems (ISCAS)*, vol. 1, 1989; 118–121.
37. Ejthvoulidis G, Toth L, Tsvividis YP. Noise in  $G_m$ -C filters. *IEEE Transactions on Circuits and Systems* 1998; **45**(3):295–302.
38. Korotkov AS, Unbehauen R. Calculation and estimation of noise in all-pole  $G_m$ -C filters. *International Journal of Electronic Communication* 1999; **53**(3):151–154.
39. Mezher KA, Bowron P. Noise-flow-graph analysis of OTA-C filters. *Proceedings of the International Symposium on Circuits and Systems (ISCAS)*, vol. 1, 2001; 695–698.
40. Fortuna Z, Macukow B, Wąsowski J. *Metody Numeryczne*. Wydawnictwa Naukowo Techniczne: Warszawa, 1993.
41. Koziel S, Schaumann R, Xiao H. Analysis and optimization of noise in continuous-time OTA-C filters. *IEEE Transactions on Circuits and Systems—I* 2005; **52**(6):1086–1094.

42. Kallam P, Sanchez Sinencio E, Karsilayan A. An enhanced adaptive Q tuning scheme for a 100 MHz fully symmetric OTA based band pass filter. *IEEE Journal of Solid-State Circuits* 2003; **38**:585–593.
43. Moschytz GS, Horn P. *Active Filter Design Handbook*. Wiley: New York, 1981.
44. Su K. *Analog Filters*. Kluwer Academic Publishers: Dordrecht, 2002.
45. Szczepanski S, Koziel S, Sánchez-Sinencio E. Linearized CMOS OTA using active-error feedforward technique. *Proceedings of the International Symposium on Circuits and Systems (ISCAS)*, vol. 1, 2004; 549–552.